Modeling multi-component transport and enhanced anaerobic dechlorination processes in a single fracture-clay matrix system

4 authors:

Julie C Chambon
Technical University of Denmark
20 PUBLICATIONS **215** CITATIONS

SEE PROFILE

Mette M Broholm
Technical University of Denmark
54 PUBLICATIONS **746** CITATIONS

SEE PROFILE

Philip J Binning
Technical University of Denmark
112 PUBLICATIONS **1,668** CITATIONS

SEE PROFILE

Poul L Bjerg
Technical University of Denmark
154 PUBLICATIONS **4,972** CITATIONS

SEE PROFILE

Modeling multi-component transport and enhanced anaerobic dechlorination processes in a single fracture–clay matrix system

Julie C. Chambon [*], Mette M. Broholm, Philip J. Binning, Poul L. Bjerg

Department of Environmental Engineering, Technical University of Denmark, Miljoevej, Building 113, 2800 Kgs. Lyngby, Denmark

ARTICLE INFO

ABSTRACT

Clayey tills contaminated with chlorinated solvents are a threat to groundwater and are difficult to remediate. A numerical model is developed for assessing leaching processes and for simulating the remediation via enhanced anaerobic dechlorination. The model simulates the transport of a contaminant in a single fracture–clay matrix system coupled with a reactive model for anaerobic dechlorination. The model takes into account microbially driven anaerobic dechlorination, where sequential Monod kinetics with competitive inhibition is used to model the reaction rates, and degradation is localized to account for potential pore size limitations on microbial entry to the clay matrix. The model is used to assess the distribution of TCE and its daughter products in the clay matrix and the concentration of the different compounds at the outlet of the fracture. The time frame for complete cleanup and the contaminant flux out of the clay system are assessed for different distributions of microbial degradation. Results from a set of scenarios show that time to remove 90% of the initial mass is halved when dechlorination occurs in a 5 cm reaction zone in the clay at the fracture–matrix interface (from 419 to 195 years) and decreases by an order of magnitude when dechlorination occurs in the entire matrix (to 32 years). The fracture spacing and the microbial parameters are shown to be the critical parameter for estimation of time frames depending on the system in question. Generally, the system is more sensitive to the physical processes, mainly diffusion in the matrix, than to the biogeochemical processes, when dechlorination is assumed to take place in a limited reaction zone only. The inclusion of sequential dechlorination in clay fracture transport models is crucial, as the contaminant flux to the aquifer will increase as a result of degradation due to the higher mobility of the formed daughter products DCE and VC. The model is used to examine the relationship between flux reduction and mass removal for fractured clay systems.

© 2009 Elsevier B.V. All rights reserved.

1. Introduction

Chlorinated solvents are wide spread subsurface contaminants and an important threat to groundwater quality. Chlorinated solvents are sparingly soluble dense non aqueous phase liquids (DNAPL) that can be long term sources of contamination to groundwater. Many contaminated sites occur in areas with fractured clay geology at the land surface (Chapman and Parker, 2005), where the released DNAPLs penetrate into preferential flow pathways formed by fractures and can then rapidly dissolve and diffuse from the fractures into the matrix (Falta, 2005). Even after the removal of the physical source from the site, the contaminant can back diffuse to the fracture network for hundreds of years, causing long-term contamination of an underlying aquifer (Harrison et al., 1992; Parker et al., 1997; Reynolds and Kueper, 2002). It is important to characterize the behavior of DNAPL sources in clay aquitards so as to be able to predict their impact on the underlying groundwater aquifers. The remediation of contaminated clayey till sites is very challenging, because of the complexity of the source, the processes taking place and the mass transfer limitations due

* Corresponding author. Tel.: +45 4525 2169; fax: +45 4593 2850.
 E-mail addresses: jcc@env.dtu.dk (J.C. Chambon), mmb@env.dtu.dk
(M.M. Broholm), pjb@env.dtu.dk (P.J. Binning), plb@env.dtu.dk (P.L. Bjerg).

to slow diffusion process in the low permeability clay matrix (Johnson et al., 1989).

This work will focus on the inclusion of Monod kinetic biodegradation models into fracture matrix transport models. The influence of the distribution of biomass will be discussed. The model will be used to predict the behavior of chlorinated solvent sources undergoing anaerobic dechlorination in fractured clay aquifers. Anaerobic dechlorination has successfully been applied for sandy aquifers (Scheutz et al., 2008), and has been suggested as a remediation technology for clayey till sites, where anaerobic dechlorination is enhanced by injection of substrate and bacteria in the source area.

Knowledge of groundwater flow and solute transport in fractured porous media has greatly improved in the last 20 years because of field experiments and mathematical modeling. Extensive fracture mapping and hydraulic experiments have shown that vertical fractures can extend to significant depths in clayey tills and can create hydraulic connection through the clay layer to the underlying aquifer (Mckay and Fredericia, 1995; Jakobsen and Klint, 1999). Tracer tests confirm the existence of preferential flow pathways in the clayey till and their importance in the characterization of solute transport (Sidle et al., 1998; Nilsson et al., 2001; Jorgensen et al., 2002).

Mathematical models complement field research and were developed to simulate flow and transport in fractured porous media (Neretnieks, 1980; Grandi and Ferreri, 1991). Sudicky and Frind (1982) developed an analytical solution for transient contaminant transport in a single fracture adjacent to a porous matrix, which was extended to include reactive transport of N-member decay chains undergoing first order sequential degradation in Sun and Buscheck (2003) and Shih (2007). Sequential anaerobic dechlorination of TCE to ethene can be simulated with these models, but they do not take into account the difference in the transport properties (sorption/diffusion) of the various daughter compounds. More complex geometries, with a network of orthogonal fractures, can also be simulated with numerical models (Sudicky and McLaren, 1992; Therrien and Sudicky, 1996).

Fracture transport models typically simulate degradation using first-order rate laws and uniform degradation in the whole system (Bodin et al., 2003; Falta, 2005). However anaerobic reductive dechlorination is a microbial driven process, which depends on specific degraders, redox conditions and electron donor availability (Duhamel et al., 2002). The sequential dechlorination of TCE to ethene is better modeled by modified Monod kinetic models, accounting for biomass growth/decay, limiting substrate conditions, the presence of competitive microbial populations, and competitive inhibition between electron acceptors (Bagley, 1998; Fennell and Gossett, 1998; Cupples et al., 2004; Yu et al., 2005). Anaerobic dechlorination is also spatially limited to the zones where the specific degraders are present. The presence of bacteria in the clay may be limited by the small pore sizes and hence limit contaminant degradation to the high permeability zones (fractures and sand lenses) (Broholm et al., 2006; Lima and Sleep, 2007).

When evaluating contaminant discharge to groundwater from clay contaminated sites, it is important to consider long term leaching and the influence of anaerobic dechlorination on mass removal. Many recent studies have focused on developing a relationship between mass removal in the source and flux reduction to the aquifer (Zhu and Sykes, 2004; Falta et al., 2005; Christ et al., 2006; DiFilippo and Brusseau, 2008; Falta, 2008). However none of these studies consider the case of anaerobic dechlorination in the source zone, with the formation of toxic daughter products.

The overall objective of this work is to develop a reactive transport model in fractured media in order to identify and characterize the controlling processes and parameters involved in depletion of a TCE-source by anaerobic dechlorination in a single fracture–matrix system. The model includes state of the art knowledge of anaerobic dechlorination kinetics and aims to simulate the leaching of TCE and its daughter products during anaerobic dechlorination using component specific transport parameters. The model is used to examine the contaminant distribution in the matrix, the contaminant flux at the fracture outlet, and the contaminant impact on an underlying aquifer.

2. Methods

2.1. Physical system

Fig. 1 illustrates a common geological setting with a fractured clayey till overlying a sand or gravel aquifer. The contaminant source is typical of old industrial sites, where the spill occurred during the 1950–70's and the physical source has now been removed, but an important contaminant mass is present in the clayey till and leaching occurs to the underlying aquifer.

The fractures shown on the figure are a simplification of the natural network; the present work focuses on downward transport from the till to the aquifer so horizontal features are neglected. For the same reason, only the fully penetrating vertical fractures are taken into account and a uniform fracture spacing is assumed. This last assumption means that symmetry in the fracture/matrix geometry can be employed so that the model only considers one half of a fracture and one half of the adjacent clay matrix (dashed line in Fig. 1b).

The contaminated zone in the clayey till is assumed to be located in the saturated zone, below the water table. This assumption is consistent with the late-time scenario considered in this work, where the system is modeled long after the spreading of the contaminant; most of the contaminant mass has reached the saturated zone and it is no longer necessary to account for the unsaturated zone. Furthermore it is assumed that the residual phase in the contaminated zone can also be neglected when considering a late-time scenario; Parker et al. (1994, 1997) have shown that the time for disappearance of DNAPL from fractures due to dissolution and diffusion into the matrix is short relative to the age of contamination at a number of contaminated sites. Hence only the dissolved and sorbed phases are modeled in this study.

2.2. Governing equations

2.2.1. Solute transport

The equations for solute transport in the half fracture–half matrix system are based on the conceptual model developed by Sudicky and Frind (1982) (Fig. 1b). Assuming that the fracture width is much smaller than its length and that transverse diffusion and dispersion within the fracture assures complete
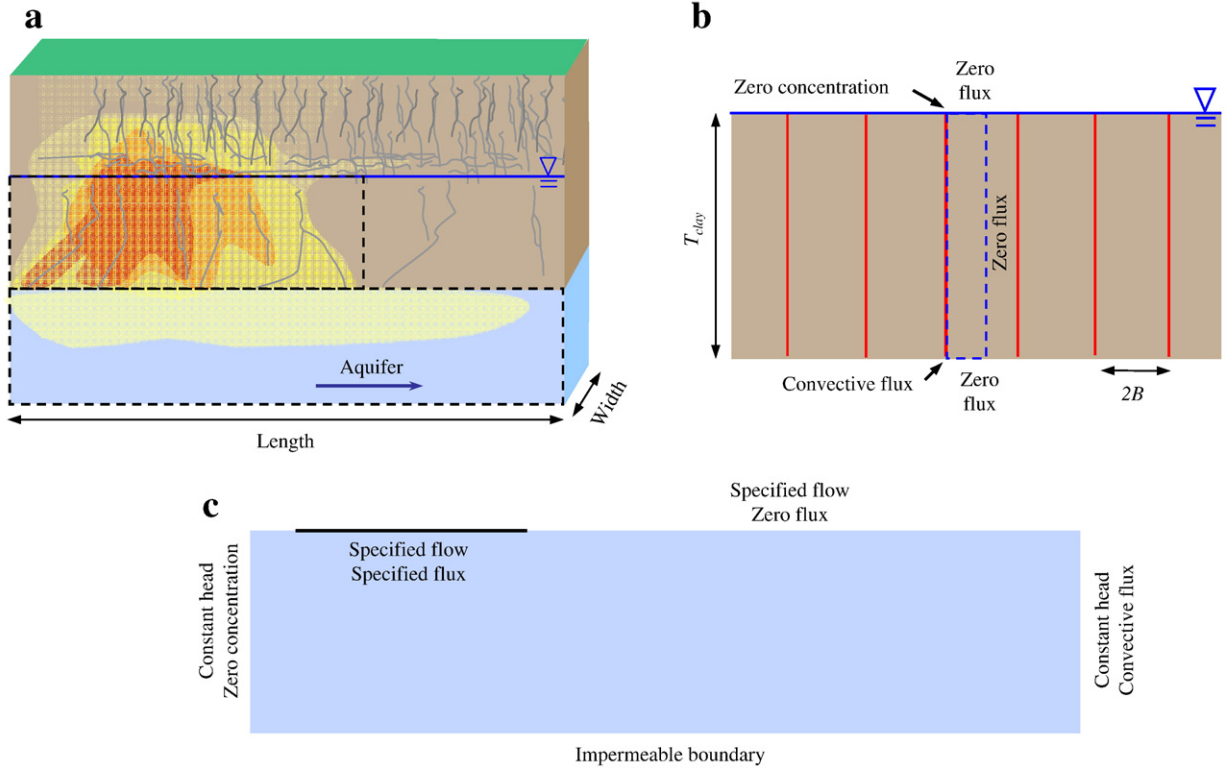
Fig. 1. a) Physical system considered in this study: a clayey till overlies an aquifer. The contamination source is mainly located in the saturated zone of the clayey till. The upper and lower dashed boxes show the areas considered in figures b) and c) respectively. b) Simplification of the clay layer for modeling: the fractures are assumed to be fully penetrating and equally spaced. The model domain (dashed line) and the boundary conditions are indicated. c) 2D cross-section of the aquifer, with the boundary conditions for the flow and solute transport models. The contamination source is represented by the solid line.

mixing across its width at all times, the transport in the fracture can be described with a one-dimensional equation (Tang et al., 1981):

$$\frac{\partial C_{f,i}}{\partial t} + v_f \frac{\partial C_{f,i}}{\partial z} - D_{f,i} \frac{\partial^2 C_{f,i}}{\partial z^2} + \frac{Q_{m,i}}{b} = \left(\frac{\partial C_{f,i}}{\partial t}\right)_{reaction} \qquad (1)$$

where $C_{f,i}$ is the aqueous concentration in the fracture of component i (M L^{-3}), v_f is the groundwater velocity in the fracture (L T^{-1}), z is the special coordinate along the fracture (L), $D_{f,i}$ is the hydrodynamic dispersion coefficient of component i (L^2 T^{-1}), $Q_{m,i}$ is the mass transfer flux at the fracture–matrix interface (M T^{-1} L^{-1}) and b is the half aperture of the fracture (L). The concentration change with time due to anaerobic dechlorination $\left(\frac{\partial C_{f,i}}{\partial t}\right)_{reaction}$ will be discussed later. The groundwater velocity in the fracture is equal to the flux and is given by Darcy's law:

$$v_f = K_f \cdot I \qquad (2)$$

where I is the hydraulic gradient along the fracture, and K_f is the fracture hydraulic conductivity (L T^{-1}) which can be calculated using the "cubic law" (Snow, 1969):

$$K_f = (2b)^2 \frac{\rho g}{12\mu} \qquad (3)$$

where ρ is the fluid density (M L^{-3}), g is the gravitational acceleration (L T^{-2}) and μ is the viscosity (M L^{-1} T^{-1}).

The water discharge in the fracture is then given by (per unit width of fracture):

$$Q_{w,f} = (2b)^3 \frac{\rho g}{12\mu} I \qquad (4)$$

The hydrodynamic dispersivity coefficient is defined as (Bear, 1972):

$$D_{f,i} = \alpha_L v_f + D_{d,i} \qquad (5)$$

where α_L is the longitudinal dispersivity (L) and $D_{d,i}$ is the free diffusion coefficient in water (L^2 T^{-1}).

Eq. (1) does not take into account adsorption on the fracture wall.

When considering contaminant transport in the matrix, it should be noted that it has a low conductivity, commonly around 10^{-10} m/s for unfractured saturated clays (Harrison et al., 1992; Jorgensen et al., 2002). Hence solute transport within the matrix is mainly by molecular diffusion and advection can be neglected. The transport in the matrix is described by the two-dimensional diffusion equation:

$$R_{m,i} \frac{\partial C_{m,i}}{\partial t} - D_{m,i} \nabla^2 C_{m,i} = \left(\frac{\partial C_{m,i}}{\partial t}\right)_{reaction} \qquad (6)$$

where $C_{m,i}$ is the aqueous concentration in the fracture of component i (M L^{-3}), R_i is the retardation factor due to sorption of component i and $D_{m,i}$ is the effective diffusion coefficient of component i (L^2 T^{-1}). The concentration change with time due to anaerobic dechlorination $\left(\frac{\partial C_{m,i}}{\partial t}\right)_{reaction}$ will be discussed later. The effective diffusion coefficient is defined as (Bear, 1972):

$$D_{m,i} = \tau D_{d,i} \tag{7}$$

where τ is the matrix tortuosity.

Linear sorption is assumed in the matrix and the retardation coefficient is defined by Freeze and Cherry (1979):

$$R_{m,i} = 1 + \frac{\rho_b}{\phi} K_{d,i} \tag{8}$$

where ρ_b is the bulk density (M L^{-3}), ϕ is the porosity of the matrix material and $K_{d,i}$ is the distribution coefficient of the component i (L^3 M^{-1}).

The coupling between the matrix and fracture equations is provided by a requirement for continuity of concentration and flux at the fracture–matrix interface where the mass transfer flux $Q_{m,i}$ at the matrix–fracture interface is defined by Fick's first law:

$$Q_{m,i} = -\phi D_{m,i} \left.\frac{\partial C_{m,i}}{\partial x}\right|_{x=b} \tag{9}$$

2.2.2. Reaction rates for anaerobic dechlorination

In presence of the specific degraders, electron donor and anaerobic redox conditions, trichloroethene (TCE) can be sequentially degraded in the aqueous phase to DCE (cis-dichloroethene), vinyl chloride (VC), and then ethene. These sequential reactions are modeled using Monod kinetics with competitive inhibition between the electron acceptors involved in dechlorination (chlorinated ethenes) for the case when electron donor (hydrogen) is non-rate-limiting (Cupples et al., 2004). Furthermore two dechlorinating biomass populations are considered: TCE dechlorinators (X_1) and DCE/VC dechlorinators (X_2), as suggested in other studies (e.g., Clapp et al., 2004; Christ and Abriola, 2007). The first dechlorinating group represents a range of dechlorinating bacteria, while the second step only involves bacteria belonging to the genus of *Dehalococcoides* (Scheutz et al., 2008).

$$\frac{dC_{TCE}}{dt} = -\frac{\mu_{TCE}{}^{X_1}/_Y c_{TCE}}{C_{TCE} + K_{TCE}\left(1 + {}^{C_{DCE}}/_{K_{i,DCE}} + {}^{C_{VC}}/_{K_{i,VC}}\right)} \tag{10}$$

$$\frac{dC_{DCE}}{dt} = -\frac{\mu_{DCE}{}^{X_1}/_Y c_{DCE}}{C_{DCE} + K_{DCE}\left(1 + {}^{C_{TCE}}/_{K_{i,TCE}} + {}^{C_{VC}}/_{K_{i,VC}}\right)} \tag{11}$$
$$+ \frac{\mu_{TCE}{}^{X_2}/_Y c_{TCE}}{C_{TCE} + K_{TCE}\left(1 + {}^{C_{DCE}}/_{K_{i,DCE}} + {}^{C_{VC}}/_{K_{i,VC}}\right)}$$

$$\frac{dC_{VC}}{dt} = -\frac{\mu_{VC}{}^{X_2}/_Y c_{VC}}{C_{VC} + K_{VC}\left(1 + {}^{C_{TCE}}/_{K_{i,TCE}} + {}^{C_{DCE}}/_{K_{i,DCE}}\right)} \tag{12}$$
$$+ \frac{\mu_{DCE}{}^{X_2}/_Y c_{DCE}}{C_{DCE} + K_{DCE}\left(1 + {}^{C_{TCE}}/_{K_{i,TCE}} + {}^{C_{VC}}/_{K_{i,VC}}\right)}$$

$$\frac{dC_{ETH}}{dt} = \frac{\mu_{VC}{}^{X_2}/_Y c_{VC}}{C_{VC} + K_{VC}\left(1 + {}^{C_{TCE}}/_{K_{i,TCE}} + {}^{C_{DCE}}/_{K_{i,DCE}}\right)} \tag{13}$$

where μ_i is the maximum growth rates on component i (T^{-1}), X_j is the biomass concentration of biomass group j (cells L^{-3}), Y is the specific yield (cells M^{-1}), C_i is the aqueous concentration of component i (M L^{-3}), K_i is the half-velocity constant of component i (M L^{-3}) and $K_{i,i}$ is the inhibition constant of component i (M L^{-3}). In Friis et al. (2007), the temperature dependence of TCE reductive dechlorination is investigated using microcosm experiments. The bottles, containing a sulfate-free mineral medium and an initial TCE concentration of 8 μmol/L, were enriched with the dechlorinating culture KB-1^{TM} and lactate or propionate was used as electron donor. The concentrations of TCE and daughter products were measured with time for the different setups. The data from the experiment performed at 10 °C, with lactate as electron donor are used to derive parameters for modeling anaerobic dechlorination (Table 1). The three growth rates, as well as K_{DCE}, are optimized whereas the others parameters are taken from the literature. The comparison with the model is shown in Fig. 2. Several similar dechlorination studies have been carried out, but at higher temperatures of 20–35 °C (Fennell and Gossett, 1998; Cupples et al., 2004; Yu et al., 2005), which are not representative of typical groundwater conditions (10–15 °C). Due to the difference in temperature and experimental conditions (culture, electron donor, culture dilution, etc.), the estimated maximum growth rates are difficult to compare, but they fall within the ranges reported in the literature.

The growth and decay of dechlorinating populations play an important role in microcosm experiments, which are typically conducting over a short time scale (100 days). In

Table 1
Parameters for the Monod kinetics model of anaerobic dechlorination.

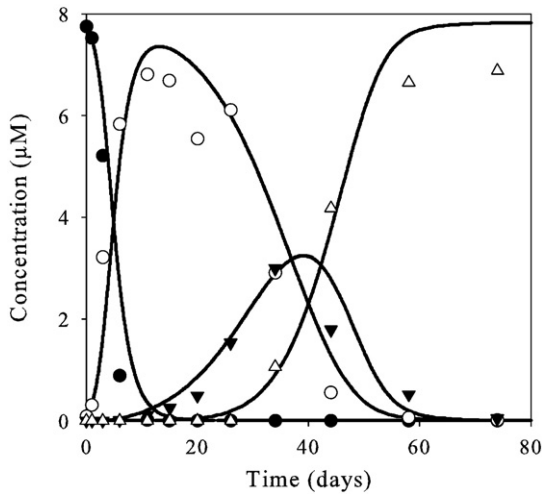|	Symbol	Values	Units	Reference
Maximum growth rate	μ_{TCE}	2	d^{-1}	Estimated
	μ_{DCE}	0.38	d^{-1}	
	μ_{VC}	0.14	d^{-1}	
Half-velocity coefficient	K_{TCE}	10	μmol L^{-1}	(Cupples et al., 2004)
	K_{DCE}	9.9	μmol L^{-1}	(except K_{DCE})
	K_{VC}	2.6	μmol L^{-1}	
Inhibition coefficient	$K_{i,TCE}$	10	μmol L^{-1}	
	$K_{i,DCE}$	3.6	μmol L^{-1}	
	$K_{i,VC}$	7.8	μmol L^{-1}	
Specific yield	Y	$5.2*10^8$	cell μmol^{-1} Cl$^-$	(Cupples et al., 2004)
Initial biomass concentration	$X_{10} = X_{20}$	10^8	cell L^{-1}	

Fig. 2. Modeled sequential anaerobic dechlorination using parameters from Table 1 (solid lines) and results from laboratory microcosm experiments from Friis et al (2007) (TCE (●), DCE (○), VC (▲) and ethene (△)). Reductive dechlorination is enhanced with KB-1™ culture and amended with lactate. The experiment was conducted at a constant temperature of 10 °C.

contrast, in situ biodegradation takes place over much longer time scales (decades up to centuries) and the bacteria populations present (or injected) can be assumed to have a constant concentration. Therefore, the mathematical model used in the following is simplified by employing constant biomass concentrations $X_1 = X_2 = 10^8$ cell L^{-1}. In case of bioremediation, where specific degraders, electron donor and nutrients are injected in the source, the microcosm studies at 10 °C are expected to be representative of the field conditions, so the derived parameters can be used in the transport model.

2.3. Dechlorination location

Clayey tills are typically heterogeneous with zones of high permeability (fractures and/or sandstringers) embedded in a low permeability matrix. Due to this high heterogeneity, the distribution of bacteria and substrate between high and low permeability zones is still uncertain, and has not yet been described for natural conditions or after enhancement by injection of substrate and/or specific degraders (bioaugmentation). Lima and Sleep (2007) showed that the migration or growth of bacteria deep within low permeability sediments is expected to be limited due to the small pore sizes, and so anaerobic dechlorination is believed to occur

mainly in the high permeability zones, where both contaminant, bacteria and substrate are present. They hypothesized that growth may occur in the clay matrix but will be limited to the zone near the interface with the high permeability zones. Limited field data seem to confirm this and indicate that microbial driven degradation can occur in the clay matrix in a reaction zone limited to few centimeters near the fracture/sandstringer interface (Broholm et al., 2006). The development of a reaction zone in the matrix may be due to the presence of micro-fractures perpendicular to the high permeability feature, enhancing the contact between bacteria, electron donor and contaminant in this region. However this mechanism has still not been experimentally documented.

In order to assess how different locations for anaerobic degradation can influence the resulting remediation time frames and the leaching of contaminant from the clay into an underlying aquifer, four different scenarios are considered in this study (see details in Table 2). Scenario a examines leaching but does not include any degradation. This is the baseline scenario. Scenario b includes degradation in the fracture, but not anywhere else. Scenario c considers degradation in the fracture and in a reaction zone, located in a 5 cm thick area of the matrix adjacent to the fracture. Finally scenario d includes degradation in the fracture and in the entire matrix. Because of the pore-size limitations, this scenario is not likely to occur, but constitutes a "best-case". For all the scenarios involving anaerobic dechlorination, the biomass concentration is assumed to be constant and the electron donor is assumed to be non-limiting.

2.4. Contamination in an underlying aquifer

The single fracture model presented in the previous section allows the simulation of the concentration of the different components at the fracture outlet. This result can be further used to assess the discharge of contaminant per unit width, to an underlying aquifer. In this case the flux from the fracture to the aquifer $Q_{i,f}$ is given by:

$$Q_{i,f} = Q_{w,f} \cdot C_{f,i}|_{z=z_{bot}} \tag{14}$$

Knowing the surface area of a square contamination source $W * W$, the contaminant discharge from the clayey till into the underlying aquifer, per unit width of source, is:

$$Q_{i,source} = Q_{i,f} \cdot \frac{W}{2B} \tag{15}$$

Table 2
Four scenarios for localization of dechlorination.

Scenarios	a	b	c	d
	Leaching only	Degradation in fracture	Degradation in fracture and reaction zone	Degradation in fracture and matrix
Degradation in fracture $\left(\frac{\partial C_{f,i}}{\partial t}\right)_{reaction}$	No 0	Yes Eqs. (10) to (13)	Yes Eqs. (10) to (13)	Yes Eqs. (10) to (13)
Degradation in matrix $\left(\frac{\partial C_{m,i}}{\partial t}\right)_{reaction}$	No 0	No 0	5 cm from the fracture interface Eqs. (10) to (13) for $x < 0.05$ m	Yes Eqs. (10) to (13)

where $2B$ is the fracture spacing (L). This definition can lead to fractional numbers of fractures in a source area, but this is a reasonable approximation given the simplified conceptual model used in this study.

In order to assess the plume development in the aquifer before, during and after remediation efforts, the aquifer is simulated with a vertical cross-section model, where the overlying clay system acts as a contamination source for the aquifer. The model considers two-dimensional steady flow coupled with a two-dimensional advection and dispersion solute transport equation. Given the long time scale of contaminant leaching from the clay system (several hundreds of years, see Results section) compared with the relatively fast transport time in the groundwater (typically 10–100 m per year), the solute transport in the underlying aquifer is assumed to be at steady state. This is equivalent to assuming that the contaminant flux from the source varies very slowly compared to the residence time in the aquifer.

The flow in the aquifer is modeled with specified head boundaries on the left and right sides, a no flow boundary at the bottom and a specified flow boundary at the top, with flow equal to the recharge rate N (L T^{-1}):

$$N = \frac{Q_{\text{w,f}}}{2B} \tag{16}$$

Assuming no adsorption and no decay in the aquifer, the governing equation for steady state transport is:

$$\boldsymbol{v}\cdot\nabla C_{\text{aq},i} = \boldsymbol{D}\cdot\nabla^2 C_{\text{aq},i} \tag{17}$$

where $\boldsymbol{v}$ is the pore water velocity from the flow simulation (L T^{-1}) and $\boldsymbol{D}$ is the dispersion tensor (L^2 T^{-1}). The dispersion in the system is insensitive at steady state to the longitudinal dispersivity (Maier and Grathwohl, 2006; Prommer et al., 2006) and the molecular diffusion is neglected, so that the dispersion tensor can be written:

$$D_{ij} = \alpha_T |v|\delta_{ij} - \alpha_T \frac{v_i v_j}{|v|} \tag{18}$$

where α_T is the transverse dispersivity (L) and δ_{ij} is the Kronecker's delta.

The boundary conditions consist of a third-type boundary along the top of the aquifer. Solute mass enters only along the source area W, where the flux is equal to $Q_{i,\text{source}}$. Outside this source area, the contaminant mass flux is zero. The water entering the aquifer on the left side is devoid of contaminant and so it is represented by a zero concentration boundary. A zero-gradient boundary condition is defined for the right-hand side and a no-flux boundary is specified for the bottom of the aquifer.

The concentration change in the aquifer along a vertical profile at a distance L from the source is modeled to relate the remediation efforts (mass removal and flux reduction) to the effects on contamination in the aquifer. In this work L is taken equal to 100 m. These concentrations can be compared with maximum concentration levels (MCL).

2.5. Numerical formulation

The single fracture model is implemented in the finite-element software Comsol Multiphysics 3.4. The matrix is represented by Eq. (6) on a rectangular area, whose width and height are equal to half fracture spacing (B) and thickness of the clayey layer respectively (T_{clay} (L)). The left-hand side represents the half-fracture, and Eq. (1) is defined on this boundary using the weak form module of Multiphysics 3.4. The variables for the two domains are expressed separately ($C_{m,i}$ and $C_{f,i}$) and the two equations are coupled by the mass transfer term in Eq. (1) and by assigning a first type boundary condition to the interface with $C_{m,i} = C_{f,i}$. Along the three other sides, the contaminant mass flux is zero. To account for the clean water entering the fracture, the top left-hand corner is defined with a zero concentration weak constraint. Steep gradients are expected at the matrix-fracture interface so the mesh is refined along this boundary.

The model discretization consists of 1861 triangle elements with localized grid refinement at the fracture–matrix boundary. Timestepping is controlled automatically by the error control system in Multiphysics. Run times for the simulations shown in this paper are approximately 40 seconds on a Intel Core 2 Duo processor 3.00 GHz with 3 GB RAM. For scenario d (the most computing demanding), the model requires 125 time steps (max time step = 2 years) for 50 years of simulation, whereas 84 time steps (max time step = 50 years) are necessary to simulate 1000 years for scenario a.

The solute transport parameters are summarized in Table 3. The transport parameters (sorption and diffusion coefficients) are typical for chlorinated solvents, whereas the geometric (fracture spacing, aperture, clay thickness) and physical parameters (bulk density, porosity, tortuosity) are taken to be representative of typical clayey till formations: vertical fracture spacings of about 1 meter are expected at 5 m below surface (Jorgensen et al., 2003); and a fracture aperture of 25 µm corresponds to a bulk hydraulic conductivity of the clayey till of 10^{-8} m/s, which is a typical value for a fractured clay formation (Fredericia, 1990). The kinetic parameters from Table 1 are used for the scenarios with anaerobic dechlorination (b, c, d).

The Multiphysics numerical model results agree with the analytical solution of Sudicky and Frind (1982) for scenario d, when a first-order degradation rate for TCE is employed and the formation of daughter products is not considered. Due to a lack of more general analytical solutions and documented benchmark models, it is not possible to independently verify the results of the full model.

The model for the aquifer is also implemented in Comsol Multiphysics, with a refined mesh along the source area. The parameters for flow and solute transport are summarized in Table 4. The hydraulic conductivity and effective porosity are typical for Danish sandy aquifers.

3. Results

3.1. Impact of the dechlorination scenarios

The four dechlorination scenarios are applied with the transport and biogeochemical parameters shown in Tables 1 and 3. At time zero, the contaminant source is composed of TCE only with an initial homogeneous aqueous concentration of 10 mg/L and no dechlorination is assumed to have occurred naturally before this time. This concentration corresponds to an initial total mass of 72 g per fracture and per unit source width (parallel to fracture direction). The set up is inspired by

Table 3
Parameters for solute transport simulation in single fracture model.

Parameters	Symbol	Value	Unit	Reference
Clay layer thickness	T_{clay}	5	m	
Fracture spacing	$2B$	1	m	(Jorgensen et al., 2003)
Fracture aperture	$2b$	25	μm	(Mckay et al., 1993)
Vertical hydraulic gradient	I	0.1	–	
Water velocity in fracture	v_f	1185	m y^{-1}	Calculated with Eqs. (2) and (3)
Water flow in fracture	$Q_{w,f}$	0.03	m^3 y^{-1} m^{-1}	Calculated with Eq. (4)
Sorption coefficient [a]	$K_{d,TCE}$	0.6	L kg^{-1}	K_{oc} values from (Abdul et al., 1987)
	$K_{d,DCE}$	0.12	L kg^{-1}	
	$K_{d,VC}$	0.05	L kg^{-1}	
Dry bulk density	ρ_b	1.9	kg L^{-1}	(Jorgensen et al., 1998)
Matrix porosity	ϕ	0.3	–	
Matrix tortuosity	τ	0.3	–	$\tau = \phi$ (Parker et al., 1994)
Longitudinal dispersivity in fracture	α_L	0.1	m	assumed
Free diffusion coefficient for 10 °C	$D_{d,TCE}$	0.020	m^2 y^{-1}	(Hayduk and Laudie, 1974)
	$D_{d,DCE}$	0.022	m^2 y^{-1}	(Lyman et al., 1990)
	$D_{d,VC}$	0.026	m^2 y^{-1}	

[a] Calculated with $f_{oc} = 1\%$ (Honning et al., 2007a).

three Danish sites contaminated with chlorinated ethenes in similar concentration ranges. The change of contaminant distribution in the matrix with time is shown in Fig. 3 for scenario a. The contaminant is flushed out of the system by the clean water entering the fracture in the top-left corner.

The source depletion as a function of time is compared for the different scenarios in Fig. 4. In this figure, ethene is not accounted for in the total mass; only the chlorinated compounds (TCE, DCE and VC) are included in the calculation. As can be seen, the scenario with degradation in the fracture only (scenario b) does not visibly differ from the scenario without degradation (scenario a). This is due to the fact that the contaminant residence time in the fracture (from 0.0015 to 0.0045 year) is controlled by the groundwater velocity and is much smaller than the degradation time (from 0.6 to 0.1 year). In contrast, source depletion is much faster when dechlorination also occurs in the matrix (within a limited reaction zone, or throughout the clay layer); the cleanup time (to remove 90% of the initial mass) in scenario c is half that of scenario a (419 and 195 years respectively), and is 13 times faster when dechlorination occurs in the whole matrix (32 years). The localization of dechlorination is therefore crucial to assess cleanup time frames. The timeframes for scenario a and d are of the same order of magnitude as results obtained by Falta (2005). He considered a similar system,

but did not consider the formation of daughter products or spatially limited degradation as seen in scenarios b and c. The results highlight that with the given set up (fracture spacing of 1 m and injection of bacteria and substrate in the vertical fracture only), a remediation scheme based on enhanced anaerobic dechlorination is only viable within a realistic timescale, if a reaction zone can develop inside the matrix or degradation can occur in the entire matrix.

Table 4
Parameters for flow and solute transport in the aquifer.

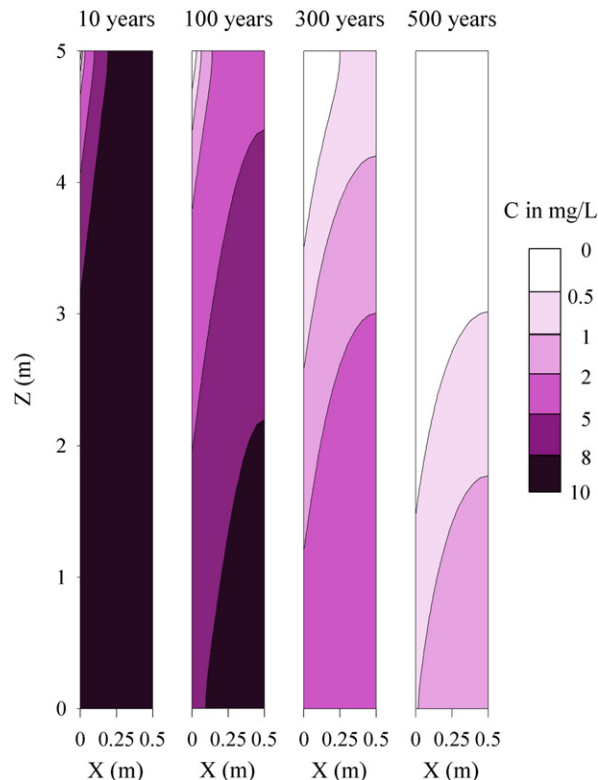| Parameters	Symbol	Value	Unit	Reference
Aquifer thickness	$T_{aquifer}$	10	m	
Hydraulic conductivity	K_{aq}	10^{-5}	m s^{-1}	
Horizontal hydraulic gradient	I_{aq}	0.01	–	
Effective porosity	Φ_{aq}	0.3	–	
Longitudinal dispersivity	α_L	Insensitive	m	Steady-state (Prommer et al., 2006)
Vertical transverse dispersivity	α_T	0.005	m	(Hojberg et al., 2005)
Source width	W	10	m	

Fig. 3. Change in contaminant distribution (aqueous concentration) with time for scenario a (no dechlorination). The fracture is located on the left-hand side.
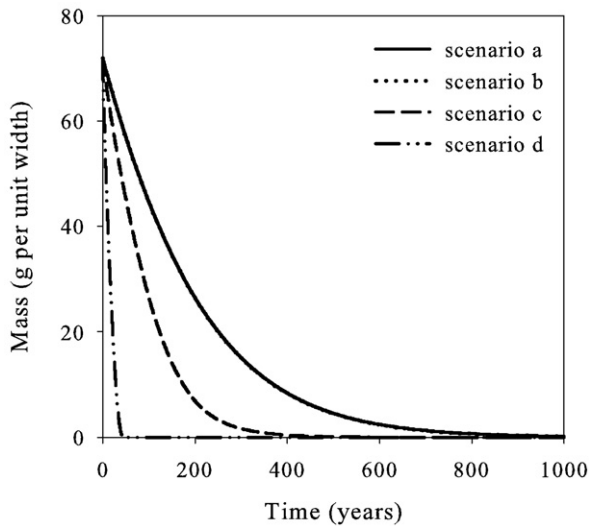
Fig. 4. Source zone mass per unit width for each fracture for chlorinated ethenes (TCE, DCE and VC). The compounds are converted from molar to mass units and summed on mass basis. Note that there is no visible difference between scenario a and scenario b.

Fig. 5. Total contaminant flux (TCE + DCE + VC) per unit width at the fracture outlet ($z = 0$). The flux is calculated from the concentration at the outlet using Eq. (14). The compounds are converted from molar to mass units and summed on mass basis. Note that there is no visible difference between scenario a and scenario b.

A key parameter in risk assessment is the contaminant flux at the fracture outlet, as shown in Fig. 5. Interestingly, the flux increases over a period of 22 and 13 years respectively, when dechlorination occurs in the matrix (either in a reaction zone (scenario c) or in the whole matrix (scenario d)). This contrasts with scenario a (leaching, no degradation) where the flux decreases monotonically with decreasing mass. The increase in flux in scenarios c and d is due to the production of daughter products (DCE and VC) which have a higher mobility in the matrix than TCE. In Fig. 6 VC is the dominant product at the fracture outlet for a long period, in contrast to the data from the microcosm experiment where no transport was considered (Fig. 2). These results illustrate that the daughter products are more mobile in the matrix than their parent products because of the higher diffusion coefficients and lower sorption coefficients shown in Table 3. The total concentration of chlorinated compounds in the aqueous phase increases with dechlorination of the contamination mass. The effect of anaerobic dechlorination is therefore to increase contaminant leaching to the underlying aquifer in the initial period following the start of degradation. This poses a threat to underlying aquifers, especially considering the formation of vinyl chloride, which is the most toxic of the chlorinated solvents and is a proven carcinogen (Kielhorn et al., 2000).

Reductive anaerobic dechlorination has been mainly used in high permeability media (like sand), where sorption and diffusion are not key processes for solute transport, and enhanced transport of daughter products has not been observed at such sites. However enhanced anaerobic dechlorination has been implemented in clayey till at Gammel Kongevej in Denmark (Kjærsgaard et al., 2006), providing an opportunity to make a qualitative comparison with the model results. The contamination hotspot at this site was located mainly in the saturated clayey till, which overlies a chalk regional aquifer (at 10 m depth). The main contaminant was TCE. Anaerobic dechlorination was enhanced with injection of molasses and
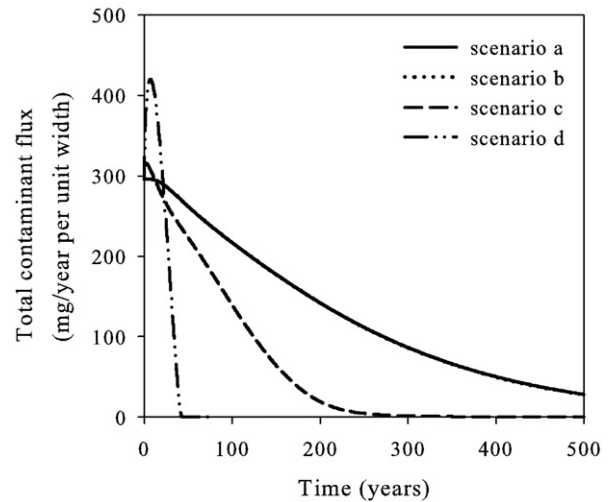
specific degraders (including bacteria of the genus *Dehalococcoides*) in the contaminated zone in the clay layer. The concentration of chlorinated solvents is monitored both in the treatment zone and the underlying chalk aquifer.

A clear shift from TCE to DCE/VC was observed in both water samples from the contaminant source area (Fig. 7a) and in the underlying aquifer (Fig. 8a), indicating that anaerobic dechlorination occurs. The total aqueous concentrations (sum of chlorinated compounds) monitored during two years after the injection are shown for the clayey till (Fig. 7b) and the underlying aquifer (Fig. 8b). An increase in the total aqueous concentrations of chlorinated solvents is observed in most of the boreholes in the treatment zone and in the
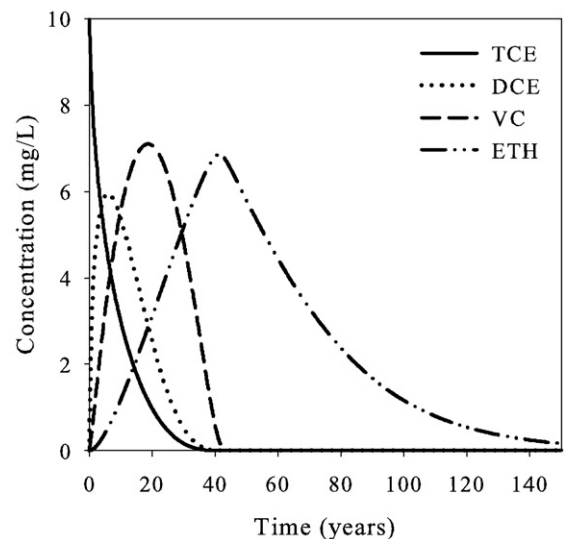

Fig. 6. Concentration of chlorinated ethenes (TCE, DCE, VC and ethene) at the fracture outlet for scenario d (degradation in matrix and fracture).

underlying aquifer. It is hypothesized that the increase is due to the higher mobility of the degradation products formed (cis-DCE, VC), compared to the parent product (TCE). The difference between the boreholes in the treatment zone is possibly due to local heterogeneities in the clayey till. In the underlying aquifer, B104 is located below the contamination source, B101 and B103 are located 2 and 10 m downstream respectively, and B29 is located 40–50 m downstream.

The results from this field site tend to qualitatively support the findings of the model, although some uncertain-
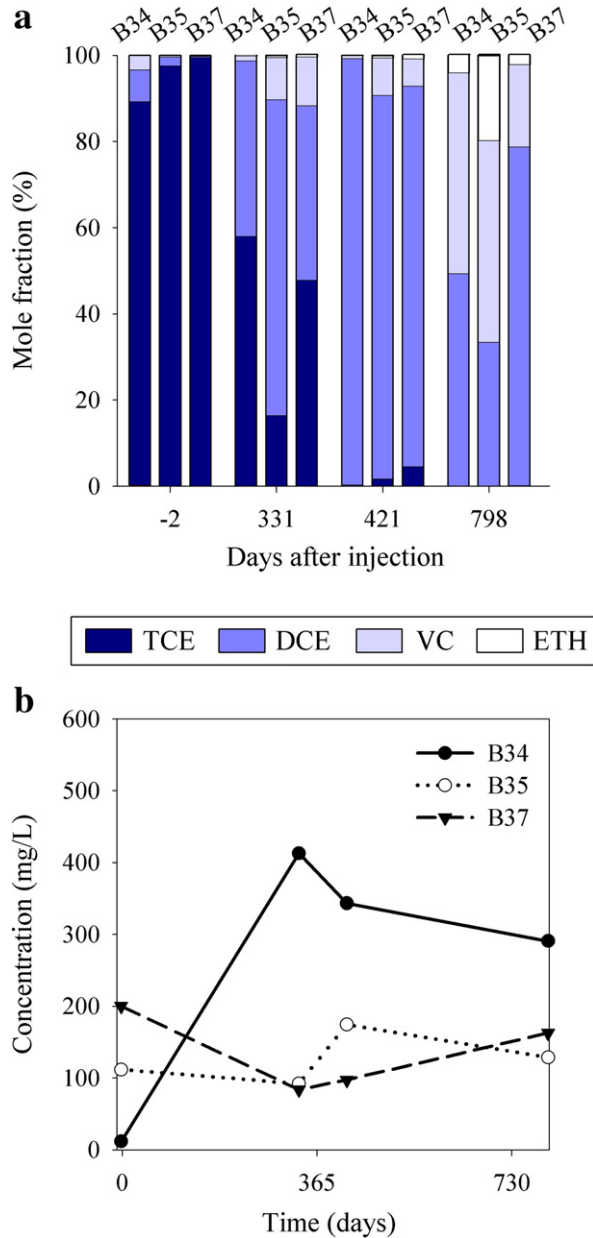

Fig. 7. Data from a clay till at a contaminated site at time − 2, 331, 421 and 798 days where anaerobic dechlorination was enhanced by injection of molasses and specific degraders at day 0. a) Mole fraction with time for boreholes B34, B35 and B37. b) Total aqueous concentration of chlorinated ethenes (TCE, DCE, VC).
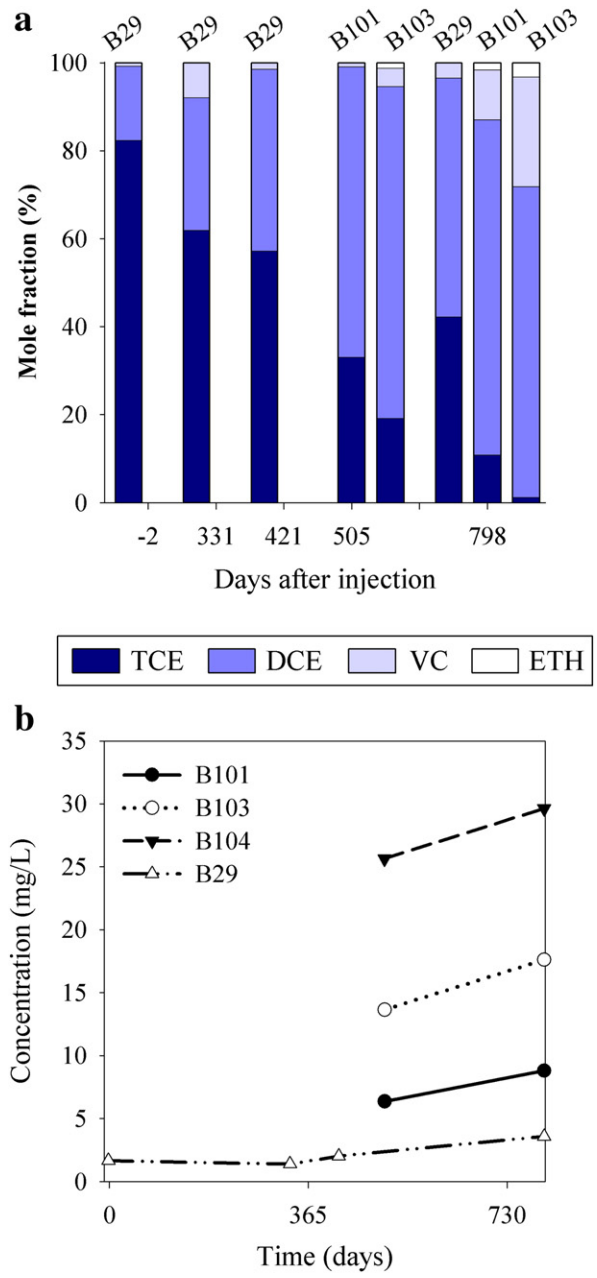

Fig. 8. Data from the underlying aquifer at a contaminated site at time − 2, 331, 421, 505 and 798 days where anaerobic dechlorination was enhanced in overlying clayey till by injection of molasses and degraders at day 0. a) Mole fraction for boreholes B29, B101 and B103. b) Total aqueous concentration of chlorinated ethenes.

ties remain on the origin of the increased concentrations observed after enhancement of anaerobic dechlorination at the site. Further laboratory and field data are needed to fully validate the conceptual model.

3.2. Relationship between contaminant discharge and mass removal

Recently several researchers have used a simple analytical model to analyze contaminant discharge from a heterogeneous

DNAPL source (Zhu and Sykes, 2004; Falta et al., 2005; Christ et al., 2006; DiFilippo and Brusseau, 2008; Falta, 2008). In this simple model, the average contaminant discharge from the source zone is a power function of the contaminant mass remaining in the source zone:

$$\frac{C(t)}{C_0} = \left(\frac{M(t)}{M_0}\right)^{\Gamma} \tag{19}$$

where C_0 is the initial concentration discharging from the source, and M_0 is the initial contaminant mass present in the source. The exponent Γ is an empirical parameter, which depends on source architecture, flow-field dynamics, and mass-transfer processes. Although this relationship was primarily developed for DNAPL source, it is expected to be applicable to a wide range of contaminants (Falta, 2008). The analytical model is intended to represent heterogeneous sources, such as fractured media.

When considering TCE only, Γ can be adjusted so that the power function matches the modeling results (as shown in (Falta, 2005)). However for the sum of chlorinated solvents, it is not possible to fit the mass-flux-reduction/mass-removal model from Eq. (19) (Fig. 9). In this case, when degradation occurs, the concentration in the fracture outlet increases as the mass decreases from M_0, due to the higher mobility of the daughter products (scenarios c and d). The maximal contaminant discharge reaches 150% of its initial value after removal of 30% of the initial mass. When daughter products are considered, the simple relationship (Eq. (19)) for the prediction of leaching behavior from source removal can be misleading. The formation of daughter products in the source zone was not considered in the studies performed by and Zhu and Sykes (2004) and Falta et al. (2005), where a simple decay was assumed for the source zone.

3.3. Plume development in the underlying aquifer

The steady state model for flow and solute transport in the underlying aquifer is run with the parameters from Table 4 and results in the contaminant distribution shown in Fig. 10. The contaminant flux from the fractured clay till dilutes quickly in the underlying aquifer, and the concentration decreases to 10% of the fracture outlet concentration at a horizontal distance of 35 m from the source. Considering a point of compliance, located 100 m downstream of the source (red line in Fig. 10), the maximum concentration observed is 5% of the concentration exiting the fracture, while the average concentration, which reflects the concentration that would be seen in a fully screened observation well, is 1% of the initial fracture concentration. This fast dilution is explained by the relatively low infiltration rate ($N = 0.03$ m.y^{-1}) compared to the mean specific discharge in the aquifer ($K_{aq}*I_{aq} = 3$ m.y^{-1}).

By applying these dilution factors to the resulting curves from the single-fracture model, the times to reach the maximum contaminant level MCLs in the aquifer at the point of compliance are assessed for the different dechlorination scenarios. The US EPA drinking water standards for TCE, DCE and VC are 5, 70 and 2 µg/L respectively. For this aquifer configuration, the times for the groundwater at the point of compliance to meet to MCLs are summarized in Table 5, considering both the maximum concentration and the average concentration at 100 m downstream. MCLs are met three times faster when dechlorination occurs in a reaction zone of 5 cm, and 20 times faster if dechlorination occurs in the whole matrix. Although the cleanup times are shortened when anaerobic dechlorination occurs in the source zone, the production of daughter products, particularly vinyl chloride, represents a threat to groundwater quality, with concentrations at 100 m downstream the source up to 60 (scenario c) and 180 (scenario d) times higher than the MCL's in the US.

For a given contaminant flux from the fracture, the plume development in the aquifer depends mainly on the ratio between the recharge rate and the mean specific discharge, the source width and the vertical transverse dispersivity. If the
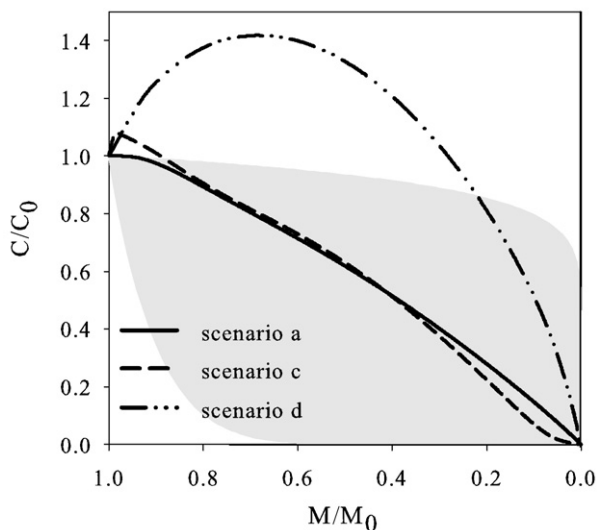

Fig. 9. Total chlorinated ethenes concentration (TCE, DCE and VC) exiting the fracture as a function of the mass remaining in the source. The shaded area indicates regions where power law relationships describe mass-flux-reduction/mass-removal for typical gamma values.
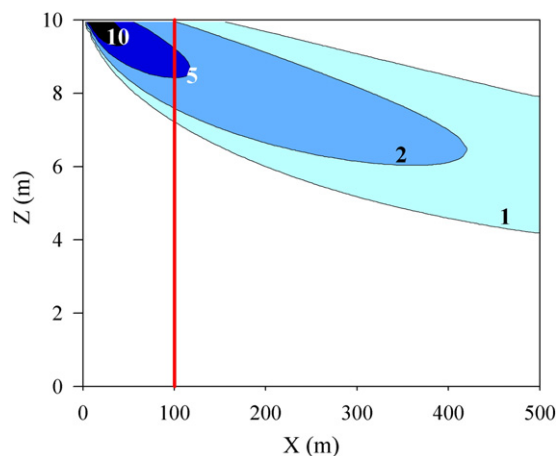

Fig. 10. Total chlorinated ethene concentrations in the aquifer as a percentage of the concentration at the fracture outlet. The point of compliance is shown by the red line.

Table 5
Time to meet the drinking water standards at 100 m downstream depending on the dechlorination scenarios.

Contaminant	Time to meet drinking standards (years)[*]		
	Scenario a	Scenario c	Scenario d
TCE	867/619	193/140	32/25
DCE	–	111/0	25/0
VC	–	290/226	43/42

*The table shows both times required for maximum concentrations and average concentrations to decrease below compliance levels.

recharge is large relative to the mean specific discharge in the aquifer, then the downstream concentrations are higher.

3.4. Sensitivity analysis

To quantify which processes and model parameters have a controlling effect on mass removal efficiency and contaminant flux reduction, the normalized sensitivity coefficients were computed (Zheng and Bennett, 2002):

$$X_{i,k} = \frac{\Delta y / y}{\Delta p_k / p_k} \quad (20)$$

where p_k is the kth parameters value, Δp_k is the perturbation of the parameter value, y is the defined dependent variable, and Δy is the change in this variable that resulted from the perturbation of parameter p_k. In order to be able to compare the results of the sensitivity analysis, the initial aqueous concentration in the matrix is adjusted as a function of the

change in parameter value (for porosity and sorption coefficients) to maintain the same initial mass in the system.

In order to reflect the influence of a parameter on both mass removal and flux reduction, two model outputs are considered, the time to remove 90% of the initial mass (t_{mass}), and the time to reach an effluent vinyl chloride concentration below 40 µg/L (t_{conc}). Vinyl chloride was chosen as the second output, as it is the chlorinated ethene with the lowest MCL. The sensitivity of the computed times to a parameter perturbation of 20% was tested for the parameters listed in Table 2 for the three dechlorination scenarios a, c and d. The comparison of the computed coefficients for mass removal is shown in Fig. 11. The corresponding sensitivity coefficients for flux reduction are similar (data not shown).

The sensitivity analysis revealed important discrepancies between the considered scenarios. While scenarios a and c are more sensitive to the transport parameters (particularly fracture aperture, fracture spacing and sorption coefficient), scenario d is more sensitive to the microbial parameters (particularly biomass concentration and specific yield). When dechlorination occurs in the whole matrix (scenario d), the system is controlled by the kinetics of the reactions. For this system, the cleanup time is mainly affected by the ratio X/Y (biomass concentration divided by specific yield), which influences all dechlorination rates (see Eq. (10) to (13)). An increase of 20% of this ratio (corresponding also to an increase of 20% of the biomass concentration) will decrease the cleanup time by 13%. By increasing the reaction rates by one order of magnitude, the cleanup time decreases by 90%, from 32 to 3.7 years. Conversely, a decrease by one order of magnitude (90%) of these reaction rates will increase the cleanup time by 300% (to 130 years). The biomass concentration at the sites can easily differ by one order of magnitude, and the high
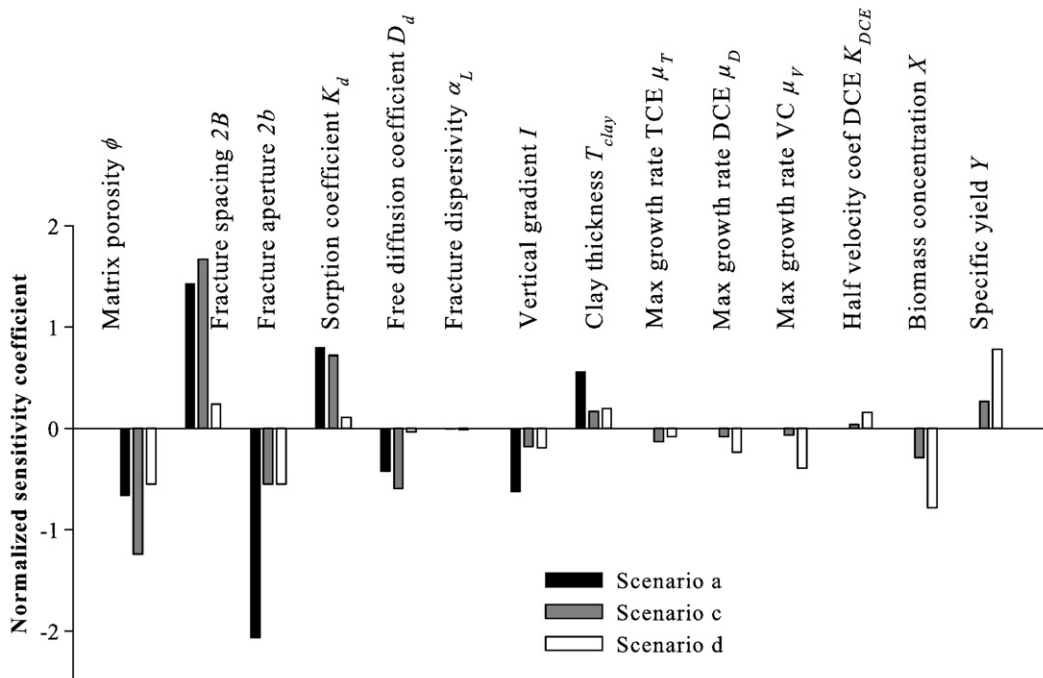

Fig. 11. Sensitivity coefficients (Eq. (20)) relative to mass removal efficiency for the three scenarios.

sensitivity of the results of scenario d to this parameter highlights the need for a site specific characterization of the biomass populations. The growth and decay of the bacteria, which was neglected in this study, may also have to be taken into account.

The system is controlled by the transport processes when dechlorination is limited to 10% of the matrix (scenario c). In this case there is a very high sensitivity to the fracture spacing ($2B$) and the porosity (Φ) and a high sensitivity to the sorption and diffusion coefficients ($K_{d,i}$ and $D_{d,i}$). These four parameters are the key parameters which control diffusive transport in the matrix. The sensitivity analysis also indicates that the mass removal efficiency for this scenario is affected by the extent of the reaction zone into the matrix.

For the natural conditions (scenario a), the system is mainly controlled by diffusion processes in the matrix with a high sensitivity to fracture spacing, sorption and diffusion coefficients, and a very high sensitivity to the fracture aperture ($2b$). The fracture aperture controls the quantity of clean water entering the fracture and flushing the contaminant (Eq. (4)). For a fixed water flow ($Q_{w,f}$) and vertical gradient (I), perturbations of $2b$ do not influence t_{mass} or t_{conc}, meaning that the aperture is not a sensitive parameter in itself, and only the quantity of water is of importance. This conclusion can also be observed in the form of the analytical solution to solute transport in a single fracture given by Tang et al. (1981).

The sensitivity analysis highlights the key processes controlling contaminant leaching from a single fracture–clay matrix system in natural conditions or when undergoing reductive dechlorination. Except for scenario d, the limiting process appears to be the back diffusion from the matrix into the fracture (scenario a) and into the reaction zone (scenario c). The transport limitations observed mean that site specific characterization is needed for the key parameters such as fracture spacing, sorption coefficients, porosity of the matrix and water flow throughout the clay unit. Some of these parameters can be difficult to measure in the field or in the laboratory, leading to relatively high uncertainties in model results. The fracture network in clayey till is, for example, currently poorly described at large depth (below 5–8 m), leading to a lack of knowledge regarding fracture spacing and aperture (Jorgensen et al., 2003).

The results show that high degradation rates in the entire matrix or narrow fracture spacings are the key to success of enhanced remediation schemes. The cleanup time frames for scenarios b and c are too long for remediation via anaerobic dechlorination to be considered viable.

4. Limitations and perspectives

The single fracture–matrix model constitutes an attempt to characterize the controlling processes and key parameters of transport in fractured clayey till combined with reductive dechlorination. The simplifications used in this study should be further investigated to overcome the limitations associated with the modeling results. We have focused attention on a homogeneous network of vertical fully penetrating fractures, which can be simplified to a single fracture matrix model; however realistic models will most likely represent heterogeneous network with horizontal features, such as fractures, sand lenses and sand stringers. Such horizontal high permeability zones are expected to play an important role in remediation by mass removal technologies (Honning et al., 2007b), because they will decrease diffusion lengths from the matrix into high conduit zones. The spreading of reactive aids like substrate and specific biomass will also be enhanced by such features (Christiansen et al., 2008). The transport of the injected electron donor from the fracture to the matrix, which will likely be limited by diffusion and interaction with the clay matrix, has not been included in this study and needs to be considered in future investigations. Further improvement of the model will therefore focus on the multiscale interaction between matrix, fracture and other high permeability features in the clayey till.

Finally, the biodegradation model employed here is quite simple with respect to the governing processes for the anaerobic dechlorination and the assumption of unlimited electron donor. The development of a more sophisticated mathematical model for sequential dechlorination, which can account for substrate production and consumption and the presence of indigenous competitive biomass populations including terminal electron acceptor processes remains a challenge. This will enable the assessment of substrate demand and the injection frequency required to maintain proper dechlorination for a specific site. Such models have been developed for conversion of xenobiotic organic compounds in complex redox environments driven by organic carbon (Prommer et al., 2006), but have not yet been developed for chlorinated ethenes or for fractured clayey till sites.

From a remediation perspective, long cleanup time frames are a major barrier to the use of enhanced reductive dechlorination in clayey till. Mass removal is mainly limited by diffusion and sorption processes in the clay matrix, and fracture spacing appears to be one of the most sensitive parameters in the model. The distance between fractures can be reduced by engineered fracturing in order to overcome the diffusion limitation and achieve cleanup within reasonable timeframes (Christiansen et al., 2008). The combination of improved injection technologies and enhanced reductive dechlorination could lead to an efficient remediation strategy for low permeability sites and should be further investigated.

5. Conclusions

A single fracture–matrix model is used to simulate anaerobic dechlorination of chlorinated solvents in fractured clay till. In this study we focused on groundwater protection by assessing the time frames for sufficient mass removal and flux reduction, given different biomass distributions inside the matrix. The model shows that this distribution greatly influences the mass removal efficiency and the contaminant leaching from the source zone; the cleanup time frames differ by one order of magnitude for the cases without and with degradation. Degradation in the matrix also results in an increase of contaminant leaching in a first period, due to the formation of more mobile daughter products such as DCE and VC. This results in a complex mass removal–flux reduction behavior that cannot be captured by a simple power function curve. Field data from a Danish site shows similar increased leaching of daughter products. The model also shows that the biomass distribution influences the factors governing the

system: fracture spacing and recharge rate are the dominant parameters in the case of no or spatially limited dechlorination, and biomass concentration is the dominant parameter in the case of uniform degradation.

The results have significant implications for the design of enhanced bioremediation schemes for clay contaminated groundwater. Remediation system design must focus on effectively encouraging widespread distribution of biomass and this is expected to be challenging in low permeability, small pore size clay system.

This study evaluates the long term impact of fractured clayey tills contaminated with chlorinated solvents on the water quality of an underlying aquifer. Future research should be conducted to characterize the kinetics of anaerobic dechlorination and the complexity of fracture networks in clay systems. It will also be relevant to apply the models to the design of reliable remediation strategies.

Acknowledgements

References

Abdul, A.S., Gibson, T.L., Rai, D.N., 1987. Statistical correlations for predicting the partition-coefficient for nonpolar organic contaminants between aquifer organic-carbon and water. Hazardous Waste & Hazardous Materials 4 (3), 211–222.

Bagley, D.M., 1998. Systematic approach for modeling tetrachloroethene biodegradation. Journal of Environmental Engineering-Asce 124 (11), 1076–1086.

Bear, J., 1972. Dynamics of fluids in porous media. Elsevier, New York.

Bodin, J., Delay, F., de Marsily, G., 2003. Solute transport in a single fracture with negligible matrix permeability: 2. mathematical formalism. Hydrogeology Journal 11 (4), 434–454.

Broholm, M.M., Scheutz, C., Begtrup, E., Bjerg, P.L., Jacobsen, C.S., Jorgensen, T., Nielsen, L., Rasmussen, P., 2006. Remediation of chlorinated solvents in clay till: importance of diffusion, in Danish. ATV Vintermøde 2006.

Chapman, S.W., Parker, B.L., 2005. Plume persistence due to aquitard back diffusion following dense nonaqueous phase liquid source removal or isolation. Water Resources Research 41 (12).

Christ, J.A., Abriola, L.M., 2007. Modeling metabolic reductive dechlorination in dense non-aqueous phase liquid source-zones. Advances in Water Resources 30 (6–7), 1547–1561.

Christ, J.A., Ramsburg, C.A., Pennell, K.D., Abriola, L.M., 2006. Estimating mass discharge from dense nonaqueous phase liquid source zones using upscaled mass transfer coefficients: an evaluation using multiphase numerical simulations. Water Resources Research 42 (11).

Christiansen, C.M., Riis, C., Christensen, S.B., Broholm, M.M., Christensen, A.G., Klint, K.E.S., Wood, J.S.A., Bauer-Gottwein, P., Bjerg, P.L., 2008. Characterization and quantification of pneumatic fracturing effects at a clay till site. Environmental Science & Technology 42 (2), 570–576.

Clapp, L.W., Semmens, M.J., Novak, P.J., Hozalski, R.M., 2004. Model for in situ perchloroethene dechlorination via membrane-delivered hydrogen. Journal of Environmental Engineering-Asce 130 (11), 1367–1381.

Cupples, A.M., Spormann, A.M., McCarty, P.L., 2004. Comparative evaluation of chloroethene dechlorination to ethene by Dehalococcoides-like micro-organisms. Environmental Science & Technology 38 (18), 4768–4774.

DiFilippo, E.L., Brusseau, M.L., 2008. Relationship between mass-flux reduction and source-zone mass removal: analysis of field data. Journal of Contaminant Hydrology 98 (1–2), 22–35.

Duhamel, M., Wehr, S.D., Yu, L., Rizvi, H., Seepersad, D., Dworatzek, S., Cox, E.E., Edwards, E.A., 2002. Comparison of anaerobic dechlorinating enrichment cultures maintained on tetrachloroethene, trichloroethene, cis-dichloroethene and vinyl chloride. Water Research 36 (17), 4193–4202.

Falta, R.W., 2005. Dissolved chemical discharge from fractured clay aquitards contaminated with DNPALs. Dynamic of Fluids and Transport in Fractured Rock. Geophysical Monograph, vol. 162. American Geophysical Union, pp. 165–174.

Falta, R.W., 2008. Methodology for comparing source and plume remediation alternatives. Ground Water 46 (2), 272–285.

Falta, R.W., Rao, P.S., Basu, N., 2005. Assessing the impacts of partial mass depletion in DNAPL source zones — I. Analytical modeling of source strength functions and plume response. Journal of Contaminant Hydrology 78 (4), 259–280.

Fennell, D.E., Gossett, J.M., 1998. Modeling the production of and competition for hydrogen in a dechlorinating culture. Environmental Science & Technology 32 (16), 2450–2460.

Fredericia, J., 1990. Saturated hydraulic conductivity of clayey tills and the role of fractures. Nordic Hydrology 21 (2), 119–132.

Freeze, R.A., Cherry, J.A., 1979. Groundwater. Prentice-Hall, Englewood Cliffs, New Jersey.

Friis, A.K., Heimann, A.C., Jakobsen, R., Albrechtsen, H.J., Cox, E., Bjerg, P.L., 2007. Temperature dependence of anaerobic TCE-dechlorination in a highly enriched Dehalococcoides-containing culture. Water Research 41 (2), 355–364.

Grandi, G.M., Ferreri, J.C., 1991. A computational method for the hydrodynamics of fractured-porous media. International Journal for Numerical Methods in Fluids 12 (3), 261–285.

Harrison, B., Sudicky, E.A., Cherry, J.A., 1992. Numerical-analysis of solute migration through fractured clayey deposits into underlying aquifers. Water Resources Research 28 (2), 515–526.

Hayduk, W., Laudie, H., 1974. Prediction of diffusion-coefficients for nonelectrolytes in dilute aqueous-solutions. Aiche Journal 20 (3), 611–615.

Hojberg, A.L., Engesgaard, P., Bjerg, P.L., 2005. Pesticide transport in an aerobic aquifer with variable pH — modeling of a field scale injection experiment. Journal of Contaminant Hydrology 78 (3), 231–255.

Honning, J., Broholm, M.M., Bjerg, P.L., 2007a. Quantification of potassium permanganate consumption and PCE oxidation in subsurface materials. Journal of Contaminant Hydrology 90 (3–4), 221–239.

Honning, J., Broholm, M.M., Bjerg, P.L., 2007b. Role of diffusion in chemical oxidation of PCE in a dual permeability system. Environmental Science & Technology 41 (24), 8426–8432.

Jakobsen, P.R., Klint, K.E., 1999. Fracture distribution and occurrence of DNAPL in a clayey lodgement till. Mass Transport in Fractured Aquifers and Aquitards, pp. 285–300.

Johnson, R.L., Cherry, J.A., Pankow, J.F., 1989. Diffusive contaminant transport in natural clay — a field example and implications for clay-lined waste-disposal sites. Environmental Science & Technology 23 (3), 340–349.

Jorgensen, P.R., Mckay, L.D., Spliid, N.H., 1998. Evaluation of chloride and pesticide transport in a fractured clayey till using large undisturbed columns and numerical modeling. Water Resources Research 34 (4), 539–553.

Jorgensen, P.R., Hoffmann, M., Kistrup, J.P., Bryde, C., Bossi, R., Villholth, K.G., 2002. Preferential flow and pesticide transport in a clay-rich till: field, laboratory, and modeling analysis. Water Resources Research 38 (11).

Jorgensen, P.R., Klint, K.E.S., Kistrup, J.P., 2003. Monitoring well interception with fractures in clayey till. Ground Water 41 (6), 772–779.

Kielhorn, J., Melber, C., Wahnschaffe, U., Aitio, A., Mangelsdorf, I., 2000. Vinyl chloride: still a cause for concern. Environmental Health Perspectives 108 (7), 579–588.

Kjærsgaard, P., Larsen, T.H., Muushardt, U., 2006. Miljøkontrollen, Gl. Kongevej 39 — Remediation planning. in Danish.

Lima, G.D., Sleep, B.E., 2007. The spatial distribution of eubacteria and archaea in sand-clay columns degrading carbon tetrachloride and methanol. Journal of Contaminant Hydrology 94, 34–48.

Lyman, W.J., Reehl, W.F., Rosenblatt, D.H., 1990. Handbook of chemical property estimation methods. American Chemical Society, Washington, DC, USA.

Maier, U., Grathwohl, P., 2006. Numerical experiments and field results on the size of steady state plumes. Journal of Contaminant Hydrology 85 (1–2), 33–52.

Mckay, L.D., Fredericia, J., 1995. Distribution, origin, and hydraulic influence of fractures in a clay-rich glacial deposit. Canadian Geotechnical Journal 32 (6), 957–975.

Mckay, L.D., Cherry, J.A., Gillham, R.W., 1993. Field experiments in a fractured clay till .1. Hydraulic conductivity and fracture aperture. Water Resources Research 29 (4), 1149–1162.

Neretnieks, I., 1980. Diffusion in the rock matrix — an important factor in radionuclide retardation. Journal of Geophysical Research 85 (NB8), 4379–4397.

Nilsson, B., Sidle, R.C., Klint, K.E., Boggild, C.E., Broholm, K., 2001. Mass transport and scale-dependent hydraulic tests in a heterogeneous glacial till-sandy aquifer system. Journal of Hydrology 243 (3–4), 162–179.

Parker, B.L., Gillham, R.W., Cherry, J.A., 1994. Diffusive disappearance of immiscible-phase organic liquids in fractured geologic media. Ground Water 32 (5), 805–820.

Parker, B.L., McWhorter, D.B., Cherry, J.A., 1997. Diffusive loss of non-aqueous phase organic solvents from idealized fracture networks in geologic media. Ground Water 35 (6), 1077–1088.

Prommer, H., Tuxen, N., Bjerg, P.L., 2006. Fringe-controlled natural attenuation of phenoxy acids in a landfill plume: integration of field-scale processes by reactive transport modeling. Environmental Science & Technology 40 (15), 4732–4738.

Reynolds, D.A., Kueper, B.H., 2002. Numerical examination of the factors controlling DNAPL migration through a single fracture. Ground Water 40 (4), 368–377.

Scheutz, C., Durant, N.D., Dennis, P., Hansen, M.H., Jorgensen, T., Jakobsen, R., Cox, E.E., Bjerg, P.L., 2008. Concurrent ethene generation and growth of Dehalococcoides containing vinyl chloride reductive dehalogenase genes during an enhanced reductive dechlorination field demonstration. Environmental Science & Technology 42 (24), 9302–9309.

Shih, D.C.F., 2007. Contaminant transport in one-dimensional single fractured media: semi-analytical solution for three-member decay chain with pulse and Heaviside input sources. Hydrological Processes 21 (16), 2135–2143.

Sidle, R.C., Nilsson, B., Hansen, M., Fredericia, J., 1998. Spatially varying hydraulic and solute transport characteristics of a fractured till determined by field tracer tests, Funen, Denmark. Water Resources Research 34 (10), 2515–2527.

Snow, D.T., 1969. Anisotropic permeability of fractured media. Water Resources Research 5 (6), 1273–1289.

Sudicky, E.A., Frind, E.O., 1982. Contaminant transport in fractured porous-media — analytical solutions for a system of parallel fractures. Water Resources Research 18 (6), 1634–1642.

Sudicky, E.A., McLaren, R.G., 1992. The Laplace transform Galerkin technique for large-scale simulation of mass-transport in discretely fractured porous formations. Water Resources Research 28 (2), 499–514.

Sun, Y.W., Buscheck, T.A., 2003. Analytical solutions for reactive transport of N-member radionuclide chains in a single fracture. Journal of Contaminant Hydrology 62 (3), 695–712.

Tang, D.H., Frind, E.O., Sudicky, E.A., 1981. Contaminant transport in fractured porous-media — analytical solution for a single fracture. Water Resources Research 17 (3), 555–564.

Therrien, R., Sudicky, E.A., 1996. Three-dimensional analysis of variably-saturated flow and solute transport in discretely-fractured porous media. Journal of Contaminant Hydrology 23 (1–2), 1–44.

Yu, S.H., Dolan, M.E., Semprini, L., 2005. Kinetics and inhibition of reductive dechlorination of chlorinated ethylenes by two different mixed cultures. Environmental Science & Technology 39 (1), 195–205.

Zheng, C., Bennett, G.D., 2002. Applied contaminant transport modeling. John Wiley & Sons, New York.

Zhu, J.T., Sykes, J.F., 2004. Simple screening models of NAPL dissolution in the subsurface. Journal of Contaminant Hydrology 72 (1–4), 245–258.